Journal of Controlled Release 401 (2027) 115555

Contents lists available at ScienceDirect

Journal of Controlled Release

journal homepage: www.elsevier.com/locate/jconrel

mRNA-LNP vaccine encoding for Fc-scaffold antigen drives FcγR-independent immunity

Shani Benarroch [a,b,c,d], Hila Cohen [e], Uri Elia [e], Yinon Levy [e], Tal Noy-Porat [e], Ronit Rosenfeld [e], David Gur [e], Ron Alcalay [e], Maya Shlosberg [a,b,c,d], Govinda Reddy Kundoor [a,b,c,d], Yahel Avraham [f], Meir Goldsmith [a,b,c,d], Erez Bar-Haim [e], Inbal Hazan-Halevy [a,b,c,d], Ofer Cohen [e], Rony Dahan [f], Emanuelle Mamroud [e], Dan Peer [a,b,c,d,*]

[a] Laboratory of Precision NanoMedicine, Shmunis School for Biomedicine and Cancer Research, George S. Wise Faculty of Life Sciences, Tel Aviv University, Tel Aviv 69978, Israel
[b] Center for Nanoscience and Nanotechnology, Tel Aviv University, Tel Aviv 69978, Israel
[c] Department of Materials Sciences and Engineering, Iby and Aladar Fleischman Faculty of Engineering, Tel Aviv University, Tel Aviv 69978, Israel
[d] Cancer Biology Research Center, Tel Aviv University, Tel Aviv 69978, Israel
[e] Department of Biochemistry and Molecular Genetics, Israel Institute for Biological Research, Ness-Ziona 76100, Israel
[f] Department of Systems Immunology, Weizmann Institute of Science, Rehovot 761000, Israel

ARTICLE INFO

Keywords:
mRNA vaccines
Lipid nanoparticles
Plague
Yersinia pestis
Fc-fusion

ABSTRACT

While clinical translation of messenger RNA (mRNA) lipid nanoparticle (LNP) technologies has redefined vaccinology, the development of potent platforms against complex bacterial pathogens is often limited by the transient expression kinetics and rapid clearance of encoded antigens. One well established approach to enhance immunogenicity is the fusion of an Fc fragment to an antigen. However, the mechanism of Fc-mediated potentiation within mRNA-LNP systems is, yet, undefined, specifically regarding the necessity of receptor-mediated interactions. Here, we demonstrate that an mRNA-LNP vaccine, encoding an Fc-fragment fused to the *Yersinia pestis* F1 antigen, drives robust protective immunity against the lethal bubonic plague by functioning as a pharmacokinetic stabilizer. Through systematic architectural design, including variation of Fc isotypes, species-matched scaffolding, and glycosylation profiling, we reveal that Fc-integration extends systemic antigen bioavailability by over 300-fold, providing a sustained kinetic window for immune priming. Remarkably, immunogenicity is preserved in Fcγ receptor (FcγR)-deficient mice, as well as with a reduced FcγR-binding Fc variant, suggesting that protective immunity is independent of classical FcγR engagement in this model. These findings decouple Fc-mediated enhancement from receptor-mediated interactions, identifying structural stabilization and prolonged persistence as the primary drivers of efficacy in mRNA-LNP vaccines. Altogether, our results provide a mechanistic framework for the design of high-potency mRNA vaccines through engineered protein stability.

1. Introduction

The global landscape of infectious disease management has been fundamentally altered by the establishment of lipid nanoparticle (LNP) encapsulated messenger RNA (mRNA) vaccines. The clinical success of this platform during the Coronavirus disease 2019 (COVID-19) pandemic highlighted the ability of mRNA-LNPs to provide fast vaccine development and scalable manufacturing [1]. Specifically, mRNA-LNP vaccines have been widely shown to induce robust humoral and cellular immune responses across diverse antigen types [2,3]. Taken together, these capabilities are valuable for countering antibiotic-resistant pathogens. While already showing success in targeting viral infections, the utility of mRNA-LNP vaccine platform in combating bacterial infectious diseases is only beginning to be explored.

Yersinia pestis, a highly virulent bacterium, is the etiologic agent of plague zoonotic disease, and a Tier 1 select agent. This gram-negative

* Corresponding author at: Laboratory of Precision NanoMedicine, Shmunis School for Biomedicine and Cancer Research, George S. Wise Faculty of Life Sciences, Tel Aviv University, Tel Aviv 69978, Israel.
E-mail address: peer@tauex.tau.ac.il (D. Peer).

https://doi.org/10.1016/j.jconrel.2026.115555
Received 10 June 2026; Received in revised form 3 November 2026; Accepted 17 November 2026
Available online 19 November 2026
0168-3659/© 2026 The Authors. Published by Elsevier B.V. This is an open access article under the CC BY-NC-ND license (http://creativecommons.org/licenses/by-nc-nd/4.0/).

bacterium has profoundly shaped human history, with its most notable outbreak being the Black Death pandemic of the 14th century. Despite the availability of antibiotic therapy, the rapid progression of bubonic and pneumonic plague, combined with the emergence of antibiotic-resistant strains, underscores the urgent need for a high-potency, rapid-response vaccine [4,5]. The F1 capsular antigen (Caf1) is a key virulence-associated factor and a major protective immunogen [6–8]. Despite its well-established immunogenicity and longstanding consideration as a leading vaccine candidate that is often formulated together with the type III secretion system component LcrV, no plague vaccine is currently approved for use in Western countries [9]. Consequently, the development of an effective preventive vaccine remains an important yet unresolved challenge in the field. To address this, we previously reported that fusing the fragment crystallizable (Fc) region of a human IgG1 antibody to a monomeric F1 antigen significantly improved the efficacy of an mRNA-LNP vaccine relative to a non-Fc-fused antigen, leading to full protection in C57BL/6 mice against the lethal bubonic form of plague disease [10].

Fc-fusion is a well-established strategy in protein therapeutics for extending half-life; the IgG Fc fragment enables neonatal Fc receptor (FcRn)-mediated recycling to prevent intracellular degradation while increasing the protein molecular weight resulting and reducing renal clearance, thereby ensuring a prolonged therapeutic window [11–18]. Beyond therapeutic applications, Fc-fused antigens have been investigated in recombinant protein and DNA vaccine platforms, where Fc fusion may enhance immunogenicity through effects on antigen stability, pharmacokinetics, and, in some cases, Fc receptor engagement. In these systems, Fc-based fusion proteins comprising an Fc domain fused to an antigen are traditionally thought to act as molecular adjuvants by targeting the antigen complex for binding Fc gamma receptors (FcγRs) on professional antigen-presenting cells (APCs) [18–20]. Furthermore, the Fc domain promotes spontaneous homodimerization, which not only enhances the structural stability of the fused antigen but also increases its functional avidity and, consequently, overall immunogenic potency [21,22]. However, although Fc-mediated enhancement has been described across multiple vaccine modalities, the extent to which FcγR-dependent mechanisms contribute to improved immunogenicity has not been uniformly established and remains incompletely understood across nucleic acid-based vaccine platforms.

In the context of mRNA-LNP vaccination, the mechanistic basis of Fc-mediated enhancement remains undefined. Consequently, it is unknown whether improved immunogenicity results primarily from FcγR-dependent targeting of antigen-presenting cells, prolonged antigen persistence, enhanced antigen stability, or a combination of these mechanisms. Indeed, our mRNA-LNP vaccine encoding an Fc-fused *Y. pestis* F1 antigen elicited antigen-specific humoral and cellular responses, providing effective protection against bubonic and pneumonic plague, underscoring the potential of combining mRNA technology with Fc fragment engineering to boost vaccine efficacy [10,23]. However, the dominant molecular basis of this effect in this platform remains unresolved.

In this study, we perform a comprehensive mechanistic dissection of the Fc-fusion to F1 antigen architecture. By evaluating diverse Fc isotypes (human IgG1, IgG4), species-matched scaffold (mouse IgG2c), and glycosylation-deficient Fc mutants (F1-hIgG1-AG, lacking N297-linked glycans), we define the parameters of Fc-mediated immunogenicity enhancement. We sought to elucidate how structural differences within the Fc fragment affect antigen expression, immune activation, and the effectiveness of protection following a lethal *Y. pestis* challenge. These vaccine designs were tested in both C57BL/6 and BALB/c inbred mice to avoid strain-bias. To further isolate the contribution of effector functions, we utilized an FcγR-deficient mouse model, allowing to determine whether effective immunity necessitates classical FcγR engagement. Our findings suggest that Fc-fusion functions predominantly as a pharmacokinetic stabilizer, providing a versatile framework for optimizing the immunogenicity of mRNA-delivered antigens.

2. Results

2.1. Design and characterization of Fc-conjugated F1 antigen mRNA-LNPs

To decouple the biochemical and immunological variables of Fc-enhanced mRNA vaccine potency, we designed a modular panel of mRNA constructs encoding the *Y. pestis* F1 monomeric antigen. Based on our previous finding that human IgG1 Fc-conjugated F1 confers full protection against bubonic plague [10], we expanded the scaffold architecture to test specific mechanistic hypotheses regarding receptor engagement and species-specific recognition by integrating three distinct Fc-fusions.

First, an a-glycosylated hIgG1 conjugated F1 (F1-hIgG1-AG) mutant was generated by introducing a triple mutation (N297G/S298G/T299A) to disrupt the conserved N-linked glycosylation motif Asn-X-Ser/Thr. This modification reduces classical Fc-mediated effector functions, such as FcγR binding and complement system activator C1q binding, while preserving the structural integrity required for FcRn-mediated recycling [24–27]. To further probe the impact of isotype-specific immune polarization, we designed an F1 antigen fused to an Fc fragment derived from the human IgG4 antibody (F1-hIgG4). Human IgG4 antibodies are widely used in approved therapeutic antibodies due to their reduced effector function, characterized by naturally lower affinity for activating FcγRs and reduce complement activation potential relative to other IgG subclasses, resulting in favorable safety profile [28]. As a distinct IgG subclass with unique functional features, F1-hIgG4 provides an additional Fc variant to assess how Fc context influences immunogenicity. Additionally, to assess whether vaccine potency may be augmented by non-self recognition of the human scaffold in a murine host, we replaced the human Fc domain with mouse IgG2c Fc domain, generating a mouse Fc-conjugated F1 antigen (F1-mIgG2c). Such non-self recognition could be hypothesized to exert an adjuvant-like effect. Based on our previous study, all mRNA constructs were designed with high guanine and cytosine (~60%) content, which has been shown to increase mRNA levels and protein expression [10,29]. Fc-conjugated F1 constructs were designed, each incorporating a mammalian signal peptide (SP) originating from human Ig kappa light chain upstream to the F1 gene (Fig. 1A).

In vitro transfection efficiency of the different Fc-conjugated F1 antigen mRNA constructs was evaluated in HeLa cells. Cell supernatant was collected 72 h post-transfection and subjected to Western blot analysis using anti-F1 antibody. The results confirmed the presence of F1-Fc fusion protein in the cell supernatant, indicating successful expression and secretion of all the F1-Fc mRNA variants in the mammalian system (Fig. 1B). To further quantify antigen secretion, F1 protein levels in the cell supernatants were measured by enzyme-linked immunosorbent assay)ELISA(72 h post-transfection (Fig. 1C). All F1-Fc variants were successfully detected, although notably lower extracellular antigen levels were observed for the F1-hIgG4 construct compared with the other Fc variants.

mRNA constructs were encapsulated in an LNPs formulation, which has been previously demonstrated to function as an effective mRNA-LNP vaccine against *Y. pestis,* ensuring efficient mRNA delivery and robust antigen expression *in vivo* (Fig. 1D-E) [10,30]. Physicochemical characterization of the different mRNA-LNPs resulted in highly uniform LNPs with a low polydispersity index (PDI), ζ potential ranging between (−4.5)-(−6.7) mV and high RNA encapsulation efficiency (>96%) as measured by dynamic light scattering. The uniform particles size distribution was further confirmed by cryo-electron microscopy (cryo-EM) analysis (Fig. 1F-J).

2.2. Enhanced antigen persistence and pharmacokinetic profiles conferred by Fc-fusion

Following *in vitro* confirmation that transfection of cells with mRNA-

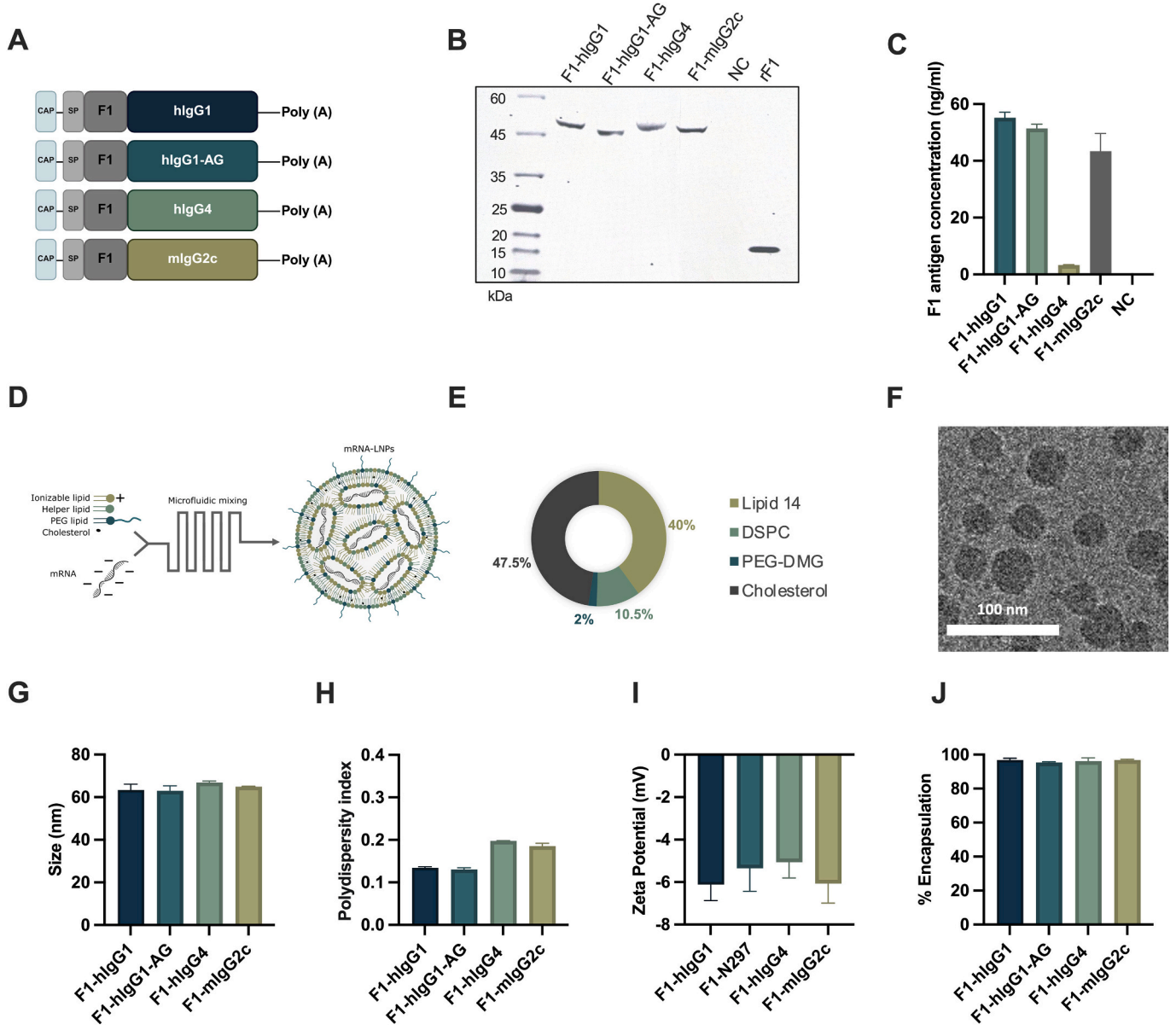


Fig. 1. Design and characterization of Fc-engineered mRNA-LNP vaccines. (A) Architectural design of mRNA constructs encoding the F1 capsular antigen. All designs include mammalian signal peptide (SP) and circularly permuted F1 (Caf1) fused to either human IgG1 (hIgG1), a-glycosylated hIgG1 (hIgG1-AG), human IgG4 (hIgG4), or mouse IgG2c (mIgG2c). (B) Western blot analysis of protein expression and secretion in HeLa cells 72 h post-transfection. Cell supernatants show successful translation and secretion across all F1-variants. Recombinant F1 (rF1) served as a positive control ($n = 3$ replicates). (C) Quantitative protein analysis of F1 antigen secretion levels in HeLa cells 72 h post-transfection measured by enzyme-linked immunosorbent assay (ELISA) ($n = 3$ replicates). Values are presented as mean ± SD. (D) Schematic representation of mRNA-LNP production using microfluidic mixing. The lipid phase (ionizable lipid, DSPC, cholesterol, and PEG-DMG) and aqueous phase (mRNA) are combined to form lipid nanoparticles. (E) LNP formulation includes ionizable lipid (lipid 14), DSPC, PEG-DMG, and cholesterol at a molar ratio of 40:10.5:2:47.5. (F) A representative cryo–electron microscopy (cryo-EM) image of LNPs. (G) LNPs hydrodynamic mean diameter (nm); (H) Polydispersity index (PDI), and (I) ζ potential (mV) as measured by Zeta Sizer. (J) Percentage of mRNA encapsulation efficiency (EE%) as measured by a RiboGreen assay ($n = 5$). Values are presented as mean ± SD.

LNPs results in efficient antigen translation, we next evaluated whether Fc-fusion alters the systemic behavior of the encoded F1 antigen *in vivo*. To directly assess the pharmacokinetic properties of Fc-fused *versus* non-fused antigens under conditions permitting reliable serum quantification, we administered the mRNA-LNPs *via* retro-orbital injection at an equal dose. This approach enabled controlled comparison of construct-dependent differences in systemic persistence, independent of local expression kinetics or tissue absorption variables. We evaluated three mRNA constructs encoding either a non-Fc fused F1 antigen (SP-F1) or Fc-fused variants incorporating human IgG1 or mouse IgG2c scaffolds (F1-hIgG1 and F1-mIgG2c), enabling direct assessment of species and isotype-specific Fc contributions to antigen stability in circulation. In a preliminary experiment, intramuscular (IM) and intravenous (IV) administration of F1-hIgG1 mRNA-LNPs were compared, revealing lower circulating antigen concentrations following IM administration. Therefore, IV administration was selected for the comparative pharmacokinetic analysis to facilitate reliable detection of circulating antigen, particularly for the non-Fc-fused SP-F1 construct (Fig. S1). Serum pharmacokinetics were then assessed in BALB/c and C57BL/6 mice following a single 20 μg retro-orbital injection of mRNA-LNP vaccines (Fig. 2A). Quantitative analysis of serum F1 concentrations measured by antigen-specific ELISA distinct circulating antigen profiles among the

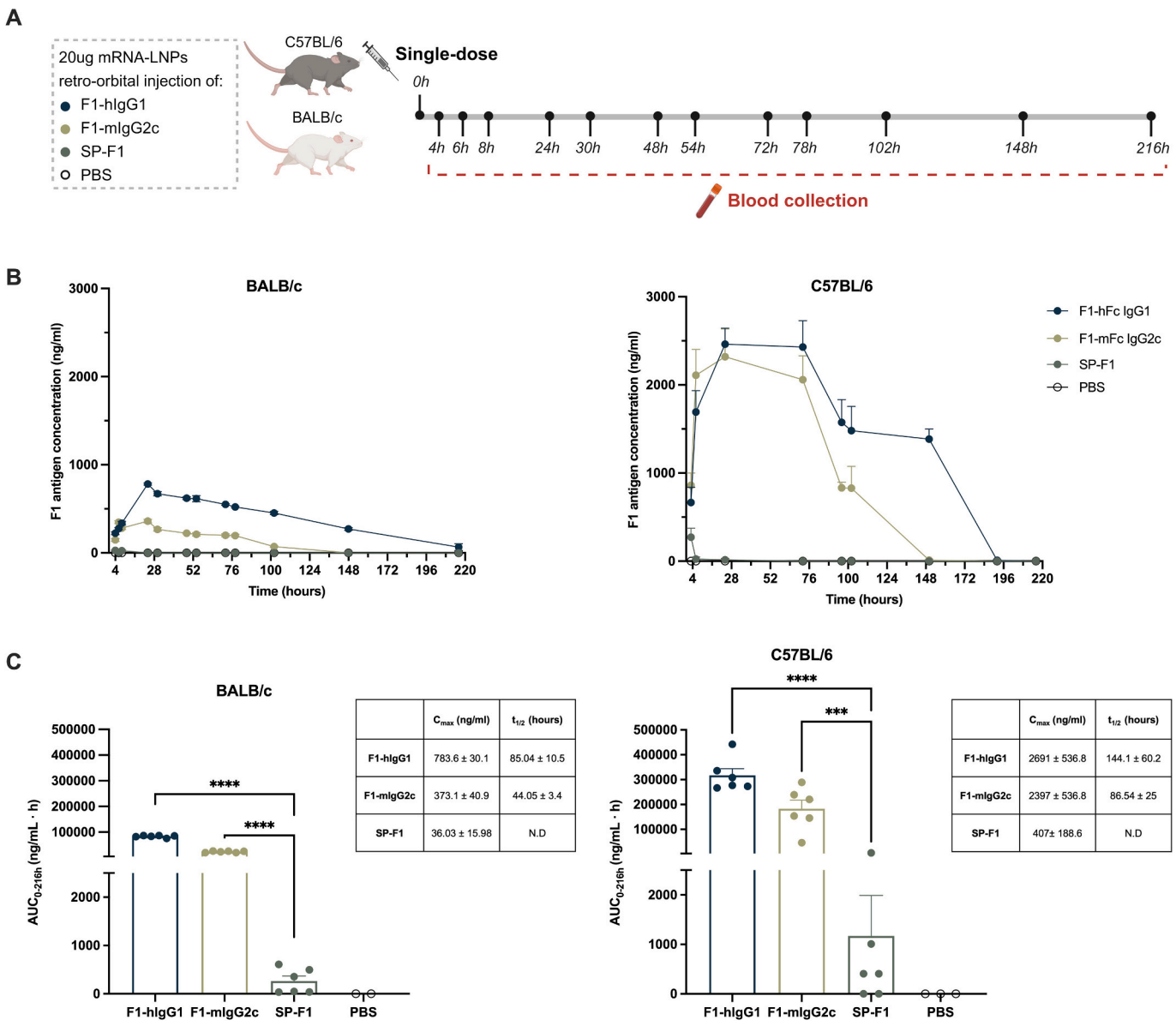


Fig. 2. Fc-fusion dictates systemic antigen pharmacokinetics. (A) Schematic representation of experimental design. BALB/c and C57BL/6 mice were immunized with a single intravenous injection (20 μg) of SP-F1, F1-hIgG1 and F1-mIgG2c mRNA-LNP vaccines ($n = 6$). (B) F1 antigen levels in mice serum were measured over 216 h using enzyme-linked immunosorbent assay (ELISA). Data points represent the mean serum concentration ± SEM. (C) Quantitative pharmacokinetic analysis of serum data. Cumulative bioavailability was calculated as the Area Under the Curve (AUC_{0-216h}). Statistical analysis was performed using a one-way ANOVA with Tukey's multiple comparisons test (****$P < 0.001$). Calculated peak concentration (C_{max}) and terminal biological half-life ($T_{1/2}$) for each group. Values are presented as mean ± SD. (N·D = Not determinable due to rapid clearance).

constructs in both mouse strains (Fig. 2B).

In BALB/c mice, mice injected with the non-fused SP-F1 construct exhibited a minimal, transient antigen peak ($C_{max} = 36.03$ ng/mL), with concentrations declining rapidly toward the limit of detection within the first 24 h. In stark contrast, both Fc-fusion constructs resulted in robust and sustained serum F1 antigen levels. The F1-hIgG1 vaccine achieved the highest peak concentration ($C_{max} = 783.6$ ng/mL) within 24 h post-injection, while the F1-mIgG2c construct reached an intermediate peak ($C_{max} = 373.1$ ng/mL) (Fig. 2C). A similar overall trend was observed in C57BL/6 mice, where both Fc-fused constructs exhibited increased circulating antigen levels compared with the non-Fc-fused SP-F1 control. Notably, higher circulating antigen concentrations were observed for both F1-hIgG1 and F1-mIgG2c in C57BL/6 mice compared with BALB/c mice. The differences in serum antigen concentrations between F1-hIgG1 and F1-mIgG2c were less pronounced in C57BL/6 mice than in BALB/c mice, suggesting that the host genetic background may influence the circulating antigen profiles of different Fc variants.

Correspondingly, Fc fusions markedly prolonged antigen persistence in circulation. The estimated apparent half-life ($t_{1/2}$) of F1-hIgG1 in BALB/c mice was approximately 85 h and 144 h in C57BL/6, whereas the rapid clearance of SP-F1 precluded reliable determination of its half-life. The F1-mIgG2c construct similarly exhibited an extended half-life relative to the non-fused control, with $t_{1/2}$ of 44 h and 86 h in BALB/c and in C57BL/6, respectively (Fig. 2C).

Consistent with the combined effects on peak concentration and clearance kinetics profiles, Fc fusion substantially increased overall antigen bioavailability. Both Fc fusions demonstrated significantly higher serum antigen levels over time compared with the SP-F1 control, with the F1-hIgG1 construct exhibiting an approximately 300-fold increase in the area under the concentration (AUC_{0-216h}) (Fig. 2D). Taken together, these results suggest that Fc-fusion substantially enhances the systemic availability and persistence of mRNA-encoded F1 antigen

across different mouse strains, while suggesting that the relative circulating antigen profiles of individual Fc variants may be influenced by the host genetic background.

2.3. Humoral and cellular immune responses elicited by F1-Fc mRNA-LNP vaccines

To evaluate the immunogenicity of the different mRNA-LNP vaccines, C57BL/6 and BALB/c mice were vaccinated intramuscularly with F1-hIgG1, F1-hIgG1-AG, F1-hIgG4 or F1-mIgG2c constructs, thrice at two-week intervals (Fig. 3A). This immunization regimen was selected to ensure robust and reproducible induction of adaptive immune responses across all vaccine constructs, while enabling comparative assessment of Fc-dependent effects on immunogenicity. All mRNA-LNP formulations proved highly immunogenic, eliciting significant anti-F1 IgG titers in both C57BL/6 and BALB/c mice after the first booster vaccination. By the third bleed, after the second booster vaccination, the total anti-F1 IgG titers increased dramatically across all groups, with each vaccine variant showing a strong immunogenic response (Fig. 3B). The enhanced immunogenicity of the F1-hIgG1 mRNA-LNP vaccine was further supported by a comparison of anti-F1 antibody titers between SP-F1 and F1-hIgG1 (Fig. S2), as previously reported [10].

Beyond the humoral response against the F1 antigen, we investigated the extent to which the Fc scaffold itself acts as an immunogen in the murine host immune system. To this end, serum anti-human Fc titers were measured in F1-hIgG1 vaccinated mice. In both mouse strains, immunization with F1-hIgG1 elicited significant serum IgG titers against the human Fc fragment (Fig. 3C). These anti-scaffold titers increased across the three blood collections, confirming that in a murine host the human Fc fragment is immunogenic and elicits a progressive anti-scaffold antibody response. Another phenomenon was observed when examining serum IgG titers against the mouse Fc domain in the species-matched F1-mIgG2c vaccine. As could be expected, BALB/c mice mounted a clear anti-mouse Fc response, since the IgG2c isotype is not natively expressed in this genetic background. Conversely, no detectable anti-mouse Fc titers were observed in C57BL/6 mice after all three doses

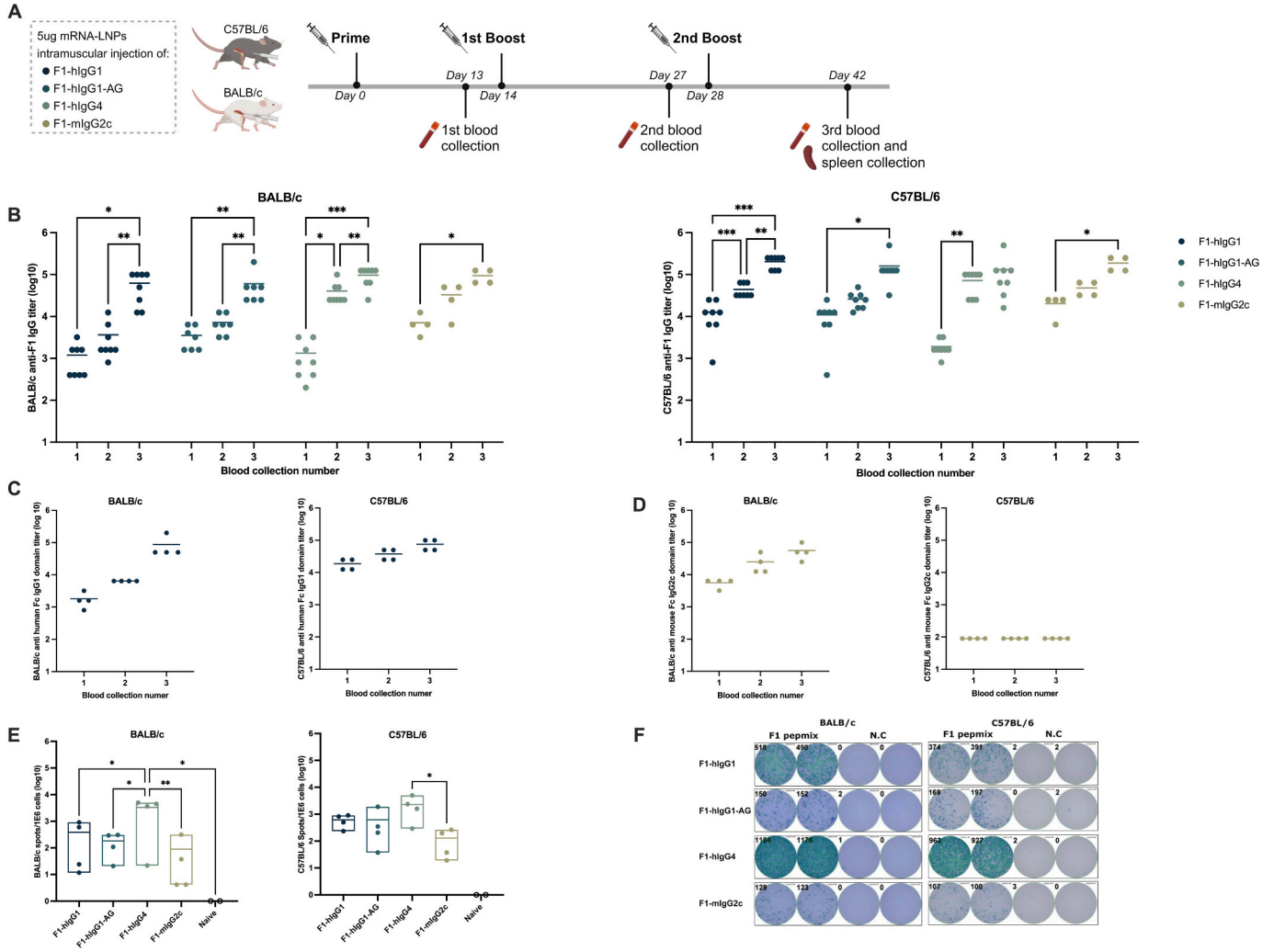


Fig. 3. Comparative F1 antigen immunogenicity and scaffold recognition. (A) Schematic representation of vaccination regimen: BALB/c and C57BL/6 mice ($n = 4$–8) were vaccinated intramuscularly with F1-hIgG1, F1-hIgG1-AG, F1-hIgG4 and F1-mIgG2c mRNA-LNP vaccines (5 μg) at days 0, 14 and 28. Blood samples were collected before each booster dose. (B) Serum samples were assayed for anti-F1 total IgG antibodies by ELISA. (C) Scaffold-specific immunogenicity was measured in BALB/c and C57BL/6 mice serum ($n = 4$): IgG titers against the human IgG1 Fc domain in mice immunized with F1-IgG1 and (D) IgG titers against the mouse IgG2c Fc domain in mice immunized with F1-mIgG2c were measured by ELISA. (E) F1-specific cellular response was determined by enzyme-linked immunosorbent spot (ELISpot). Splenocytes were stimulated with an F1 peptide library 14 days after the final vaccination. Data shows the number of spot-forming cells (SFC) per splenocyte ($n = 4$). (F) Representative wells from the ELISpot assay, used for quantification. Statistical analysis was performed using a two-way ANOVA with Tukey's multiple comparisons test (for humoral response assay) or two-way ANOVA followed by Bonferroni *post hoc* test (for cellular responses assay) (*$P < 0.05$, ** $P < 0.01$, and *** $P < 0.001$).

(Fig. 3D). In contrast to BALB/c, C57BL/6 mice naturally express the IgG2c isotype, which may result in the Fc scaffold being recognized as self, effectively avoiding anti-scaffold immunity [31]. Importantly, the magnitude of the antibody response against F1 antigen remained consistent regardless of whether the immune responses against the human or mouse Fc fragments were detected. This finding suggests that the non-self recognition of the Fc scaffold is not a requirement for high-potency humoral immunity.

To further dissect the immune profile, we characterized the cellular immune response elicited by the different mRNA-LNP vaccines by measuring IFN-γ secretion levels from splenocytes harvested 14 days after the final vaccination using the ELISpot assay (Fig. 3E and F). All Fc-variants successfully primed T-cell responses, with the hIgG4 and hIgG1 variants exhibiting particularly high frequencies of IFN-γ secreting cells. Interestingly, variations in cellular activation were detectable despite broadly comparable humoral responses across constructs following booster immunizations. These results indicate that Fc-variant composition influences the magnitude of cellular immune responses in this model. The ELISpot analyses were performed with limited sample size, which may contribute to the observed variability.

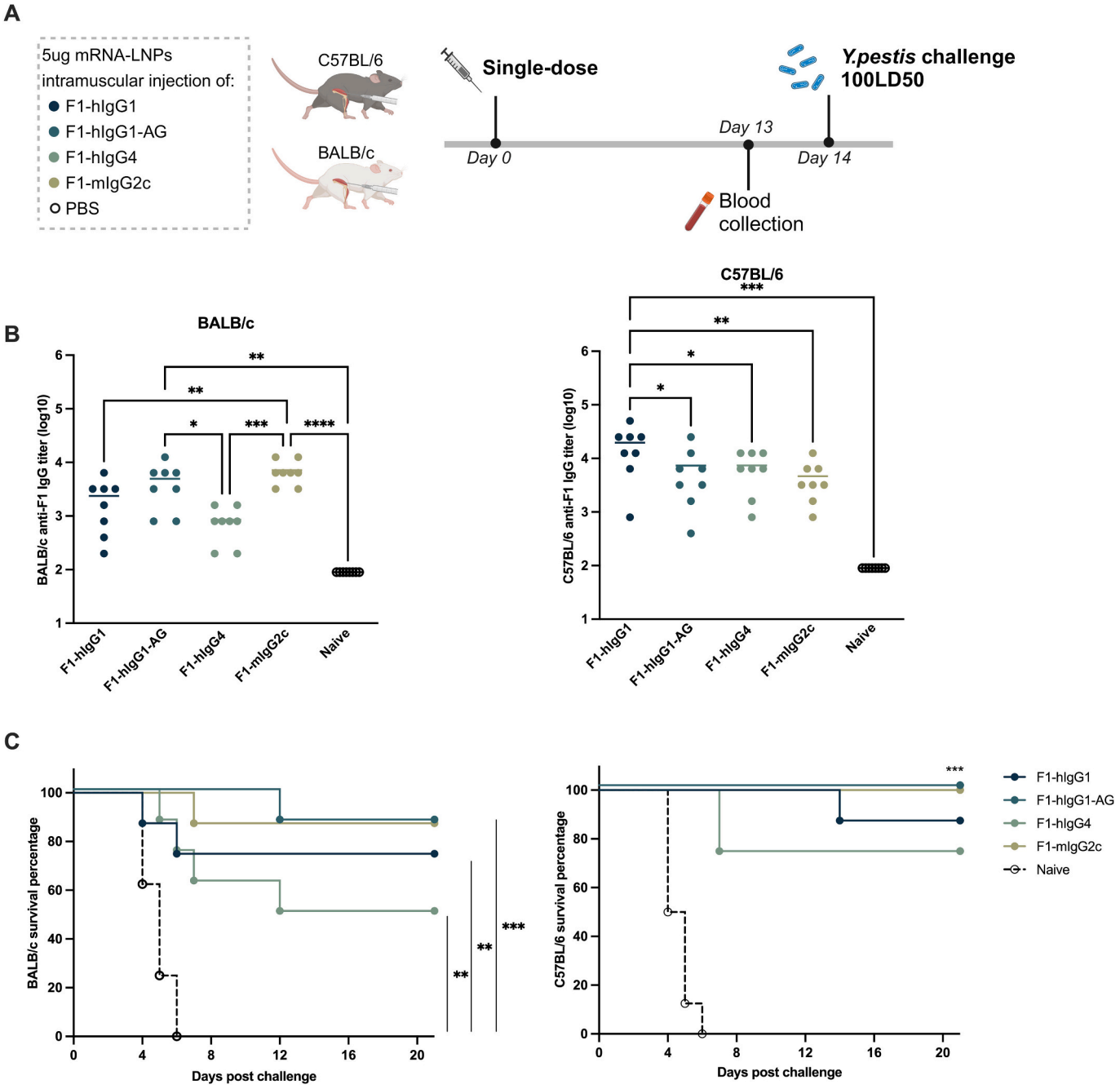


Fig. 4. Single-dose protective efficacy against the lethal *Y. pestis* challenge. (A) Schematic representation of vaccination regimen. BALB/c and C57BL/6 mice ($n = 8$) were vaccinated intramuscularly with a single dose F1-hIgG1, F1-hIgG1-AG, F1-hIgG4 and F1-mIgG2c mRNA-LNP vaccines (5 μg). (B) Blood samples were collected on day 13 and were assayed for anti-F1 total IgG antibodies by ELISA. (C) Two weeks after the vaccination, animals were subjected to a lethal ($100LD_{50}$) subcutaneous Kimberley53 challenge and monitored for survival. Statistical analysis was performed using a two-way ANOVA with Tukey's multiple comparisons test (*$P < 0.05$, **$P < 0.01$, and ***$P < 0.001$,) (for humoral response assay), or log-rank (Mantel-Cox) test (for survival plot).

2.4. Protective efficacy against the lethal bubonic Y. pestis challenge and FcγR-independent mechanisms of immunity

Considering the high immunogenicity of all mRNA-LNP vaccines, the next step was to determine whether the different F1-Fc mRNA vaccines could provide functional protection against fully virulent *Y. pestis*. Since all constructs demonstrated robust immunogenicity following a three-dose regimen, we aimed to define the protective differences by utilizing a single-dose vaccination strategy. BALB/c and C57BL/6 mice were immunized with a single 5 μg dose of the different F1-Fc mRNA-LNPs and were subcutaneously challenged two weeks post vaccination with the virulent F1-expressing *Y. pestis* Kimberley53 strain ($100LD_{50}$) (Fig. 4A). The magnitude of anti-F1 IgG responses measured in both mouse strains were consistent with protection levels (Fig. 4B). Vaccinated mice in both strains exhibited markedly improved survival compared with naïve controls, with most animals surviving the 21-day observation period (Fig. 4C). The non-Fc fused SP-F1 mRNA-LNP construct was previously shown to confer partial protection following a three-dose regimen under comparable challenge conditions, highlighting the contribution of Fc fusion to enhanced protective efficacy in this platform [10].

Mice vaccinated with F1-hIgG1 or the species-matched F1-mIgG2c exhibited high survival rates. The F1-mIgG2c construct provided comparable protection in both C57BL/6 and BALB/c mice, regardless of

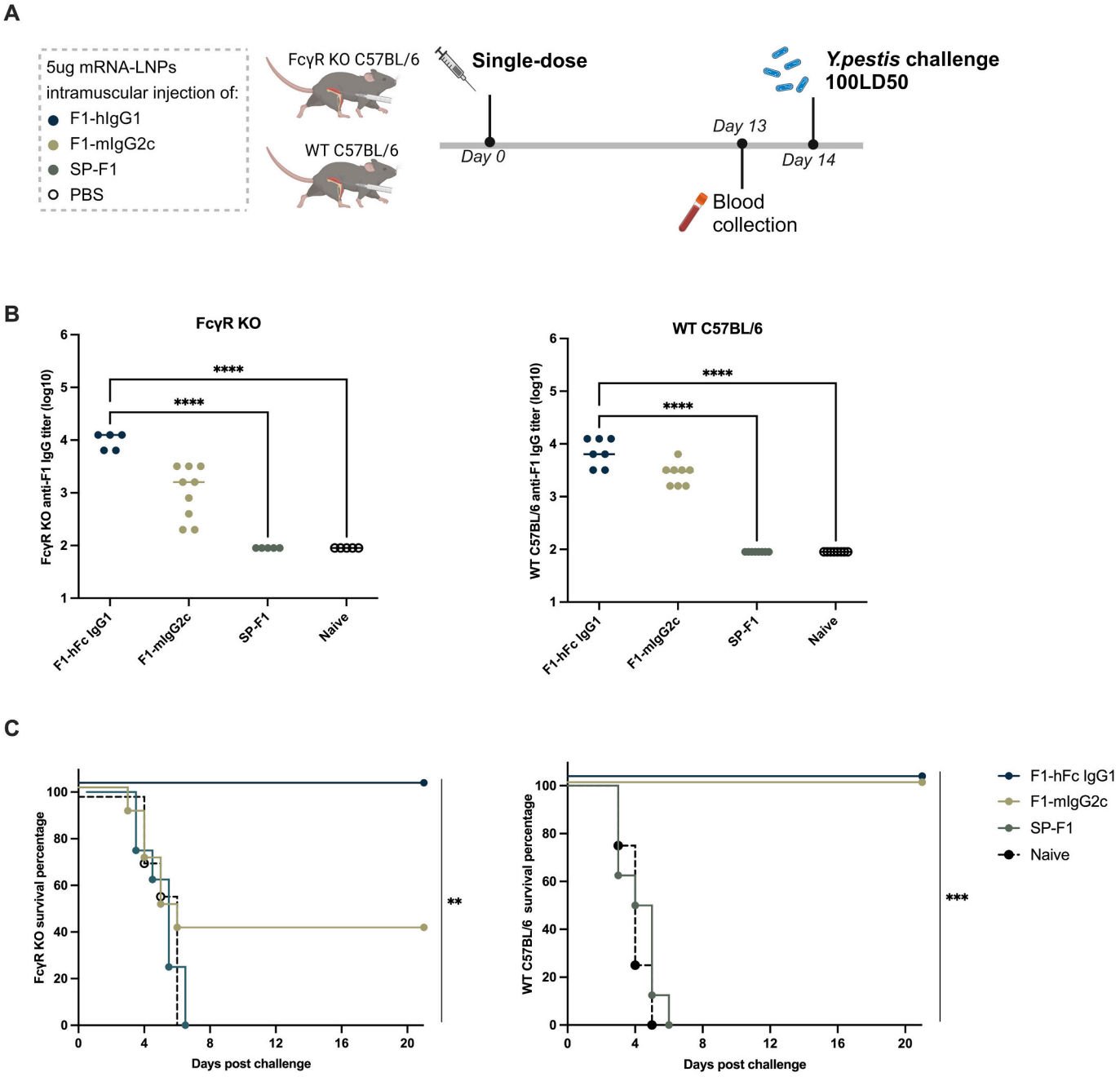


Fig. 5. FcγR -independent mechanism of vaccine-induced immunity. (A) Evaluation of FcγR requirement. Schematic representation of the single dose immunization (5 μg) in FcγR KO mice and their respective WT littermate controls (n = 5–9). (B) Serum samples were assayed 13 days post-immunization for anti-F1 total IgG antibodies by ELISA. (C) Two weeks after the vaccination, animals were subjected to a lethal ($100LD_{50}$) subcutaneous Kimberley53 challenge and monitored for survival. Statistical analysis was performed using a two-way ANOVA with Tukey's multiple comparisons test (*$P < 0.05$, **$P < 0.01$, and ***$P < 0.001$,) (for humoral response assay), or log-rank (Mantel-Cox) test (for survival plot).

whether the Fc fragment of IgG2c elicited an anti-scaffold humoral response. This parity demonstrates that while non-self recognition of the Fc fragment can provide an additional immunological stimulus, it is not a prerequisite for achieving robust protective immunity. Notably, the a-glycosylated F1-hIgG1-AG construct conferred comparable protection as the fully glycosylated IgG1 Fc construct (F1-hIgG1). Given that the F1-hIgG1-AG triple mutation is designed to substantially diminish classical FcγR engagement, this data provides an indication that the enhancement provided by Fc-fusion in our platform is not strictly dependent on FcγR-targeted antigen uptake.

The requirement for a stable Fc scaffold was further underscored by the performance of the F1-hIgG4 construct. The observed survival rate was lower compared with the other Fc-based constructs, although the difference was not statistically significant. Considering the efficacy of the FcγR-binding lower-affinity F1-hIgG1-AG mutant, this survival rate is unlikely to result from a diminished receptor engagement. Instead, the modestly lower performance of F1-hIgG4 likely reflects intrinsic structural features of the IgG4 Fc. This IgG isotype is characterized by weakened non-covalent interactions between the CH3 domains in comparison to IgG1 isotype, largely due to its unique hinge region and specific interface residues [28,32]. These properties may reduce homodimer stability and increased susceptibility to misfolding or premature degradation *in vivo*.

Our observation with the F1-hIgG1-AG mRNA-LNP vaccine suggested that the potency of the Fc-fusion platform might not be solely due to Fc-mediated effector pathways. To directly evaluate the requirement for FcγRs signaling in the immunogenicity and protective efficacy of this vaccine platform, we utilized an FcγR-deficient (FcγR KO) C57BL/6 mouse model, lacking all FcγRs. These mice, along with their wild-type (WT) C57BL/6 counterparts, were immunized with a single dose of F1-hIgG1 and F1-mIgG2c mRNA-LNP vaccine (Fig. 5A). As a negative control, we included the non-fused SP-F1 construct, which shown to elicit minimal antibody responses following a single immunization in WT C57BL/6 mice [10]. Remarkably, despite the total absence of FcγR expression, FcγR-deficient mice developed anti-F1 IgG responses following vaccination. While overall antibody levels were within a similar range to those observed in WT mice, greater inter-individual variability was noted in the FcγR KO group. Conversely, both KO and WT mice immunized with the SP-F1 control showed no detectable immune responses, further underscoring the contribution of the Fc scaffold for immune priming (Fig. 5B). To further investigate whether the preserved humoral responses translated into protective immunity, an additional challenge experiment was performed in FcγR KO mice following a single immunization with F1-hIgG1, F1-mIgG2c, or SP-F1 mRNA-LNPs. Both Fc-fused constructs previously demonstrated complete protection in WT mice, whereas distinct protective outcomes were observed in FcγR KO mice. While F1-hIgG1 maintained high protective efficacy in the absence of FcγRs, protection induced by F1-mIgG2c was reduced (40% survival). In contrast, no protection was observed in mice receiving the non-Fc-fused SP-F1 construct (Fig. 5C). These results are consistent with the findings obtained using the F1-hIgG1-AG construct and indicate that FcγR signaling is not strictly required for the induction of anti-F1 antibody responses or protective immunity following F1-hIgG1 vaccination, although the contribution of FcγR-dependent mechanisms may differ between Fc variants.

3. Discussion

In this study, we provide a comprehensive mechanistic evaluation of Fc-engineered mRNA-LNP vaccines encoding the F1 capsular antigen of *Yersinia pestis*, the causative agent of plague. Based on our previous observation that fusion of human IgG1 Fc fragment to monomeric F1 confers full protection against lethal bubonic challenge, we dissected the relative contributions of Fc isotype, glycosylation status, species matching, and FcγR engagement to vaccine performance.

A central observation of this study is the marked increase in systemic antigen exposure associated with Fc fusion. Incorporation of the Fc domain into the F1 antigen reduces its rapid renal clearance by promoting homodimerization complex which increases the molecular weight and enhances systemic retention [33]. FcRn-mediated recycling represents another possible mechanism contributing to prolonged antigen availability, as FcRn can protect Fc-containing proteins from lysosomal degradation and facilitate their return to circulation. Together, these mechanisms are consistent with the proposed role of Fc fusion in enhancing circulating antigen persistence. While the relative contributions of these pathways remain to be determined, as they were not directly investigated in the present study, our findings demonstrate increased systemic antigen exposure and prolonged circulating antigen availability following administration of Fc-fused mRNA-LNP constructs. As evidenced by the 300-fold increase in AUC for the F1-hIgG1 construct compared to the non-fused SP-F1, Fc fusion markedly increased systemic antigen exposure. This prolonged availability may provide conditions that favor iterative B-cell receptor engagement and affinity maturation required for robust protective antibody response. Accordingly, this prolonged antigen availability is expected to extend the duration of interaction with antigen-presenting cells and lymphocytes, thereby facilitating the continuous engagement of T and B cells necessary for robust immunity. Notably, the pharmacokinetic analysis performed in C57BL/6 mice demonstrated higher circulating antigen concentrations for both F1-hIgG1 and F1-mIgG2c compared with BALB/c mice. Furthermore, both constructs exhibited longer apparent half-lives in C57BL/6 mice, with estimated values of 144 and 86 h for F1-hIgG1 and F1-mIgG2c, respectively, compared with 85 and 44 h in BALB/c mice. Interestingly, although F1-hIgG1 exhibited higher circulating antigen concentrations than F1-mIgG2c in BALB/c mice, this difference was less pronounced in C57BL/6 mice. These observations suggest that host genetic background may influence the systemic profiles of Fc-fused antigens. Previous studies have reported differences in the interactions of human and murine Fc domains with mouse FcRn [34–36]. Although such interactions could contribute to the observed differences between Fc variants, FcRn binding and recycling were not directly evaluated in the present study. Nevertheless, the enhanced performance of F1-mIgG2c over non-fused SP-F1 construct, which yielded only low anti-F1 IgG titers after both prime and first booster vaccinations [10], confirms the critical contribution of Fc scaffold to antigen serum persistence and potentially supports extended immune cell interactions necessary for effective antibody responses. An additional consideration to note, the pharmacokinetic experiments involved administration of mRNA-LNPs rather than purified recombinant proteins. Consequently, circulating antigen concentrations reflect the combined effects of LNPs distribution, mRNA delivery, antigen translation, and secretion. Furthermore, the intravenous administration route and higher dose were selected to facilitate reliable serum antigen quantification, particularly for the non-Fc-fused SP-F1 construct, as supported by the preliminary comparison with intramuscular administration.

Importantly, while the pharmacokinetic analysis of serum antigen levels provides a systemic readout of Fc-mediated effects on antigen stability and circulation, circulating antigen concentrations do not necessarily directly reflect antigen availability at the primary sites of immune activation, such as the injection site, spleen or draining lymph nodes, where uptake by antigen-presenting cells and early immune priming occur. Further studies evaluating antigen distribution and cellular uptake within these tissues would be required to elucidate these mechanisms. Despite this limitation, the marked differences observed between Fc-fused and non-fused constructs remain informative, as they capture relative effects of Fc engineering on antigen persistence and degradation *in vivo*. In this context, serum antigen kinetics serve as a comparative surrogate for Fc-dependent stabilization of the secreted antigen, supporting the conclusion that Fc fusion prolongs antigen availability beyond the transient expression window of mRNA-LNP delivery.

A major consideration in Fc scaffold-based vaccine design is whether

enhanced immunity arises from non-self recognition of the human Fc fragment in a mouse model. Indeed, both BALB/c and C57BL/6 mice mounted detectable anti-human Fc responses following F1-hIgG1 immunization. Furthermore, BALB/c mice generated anti-mouse IgG2c Fc responses when immunized with the F1-mIgG2c construct, consistent with the absence of endogenous IgG2c antibody expression in that strain. The immunogenicity of heterologous Fc domains is already well established [21], yet robust anti-F1 antibody responses and protective efficacy were observed with both human and murine Fc-fused constructs, including in C57BL/6 mice, where the murine IgG2c Fc scaffold is recognized as self. These findings suggest that xenogeneic recognition is not mandatory for robust F1-specific immunity.

Beyond the impact of host recognition, intrinsic structural properties of the Fc isotype itself may contribute to the differences in protective outcomes. The comparison between F1-hIgG1 and F1-hIgG4 constructs provides an additional mechanistic insight. Interestingly, the quantitative *in vitro* ELISA analysis revealed lower extracellular F1 antigen concentrations for the F1-hIgG4 construct compared with the other Fc-fused variants. However, the F1-hIgG4 mRNA-LNP vaccine elicited robust humoral and cellular responses after multiple immunizations, and protection in a single-dose bubonic challenge was comparable to that of other Fc-based constructs, with a non-significant trend toward lower survival. These results do not indicate clear or consistent differences in protective efficacy across the Fc isotypes under the conditions tested. Structural distinctions between IgG1 and IgG4 Fc fragments, characterized by weaker CH3-CH3 domain interactions and reduced inter-chain stability in IgG4 relative to IgG1 [37], may influence antigen stability and presentation in the context of secreted Fc-fusion proteins, although the *in vivo* relevance of these effects remains to be fully defined.

A central mechanistic question underlying Fc-fusion vaccine strategies is whether enhanced immunogenicity is driven by targeting of antigen-Fc complexes to professional antigen-presenting cells *via* FcγRs. A key insight emerged from the results seen in mice vaccinated with the a-glycosylated F1-AG-hIgG1 mRNA-LNP vaccine. The N297G/S298G/T299A triple mutation disrupts the conserved Fc domain N-linked glycosylation site required for efficient binding to classical FcγR and C1q, thereby markedly reducing Fc-mediated effector functions [25,26]. Despite this impairment, F1-hIgG1-AG conferred robust immune responses and protective efficacy similar to that of the fully glycosylated IgG1 Fc fusion. The preservation of immunogenicity and protection levels in the context of markedly diminished FcγR engagement suggests that classical FcγR pathways are not the primary drivers of Fc-mediated vaccine enhancement in this mRNA-LNP platform.

To further assess the requirement for FcγR-mediated mechanisms, we evaluated vaccine performance in FcγR-deficient mice lacking classical activating and inhibitory Fcγ receptors. Indeed, immunization of FcγR KO mice with the F1-hIgG1 and F1-mIgG2c constructs resulted in a robust anti-F1 humoral response, demonstrating antibody induction can occur in the complete absence of FcγR signaling.

The protection experiment provided functional evidence, complete protection was observed in FcγR KO mice vaccinated with F1-hIgG1, whereas F1-mIgG2c provided partial protection. In contrast, no protection was observed following vaccination with the non-Fc-fused SP-F1 construct. These findings demonstrate that F1-hIgG1 can induce protective immunity in the absence of FcγRs, indicating that FcγR engagement is not a dominant requirement, and is not strictly necessary, for the enhanced immunogenicity observed in this Fc-fused mRNA-LNP vaccine model. Nonetheless, the reduced protection observed with F1-mIgG2c suggests that the contribution of FcγR-dependent mechanisms may vary between Fc variants.

Importantly, the absence of FcγRs does not preclude antigen uptake and processing by professional antigen-presenting cells, nor the recycling of the F1-mIgG2c by FcRn receptors. The secreted F1-Fc fusion complex may remain accessible to dendritic cells and macrophages through conventional endocytosis and other FcγR-independent internalization pathways. Following internalization, antigen processing and presentation through MHC class II molecules could $CD4^+$ T-cell activation and subsequent B-cell responses. Furthermore, endogenous antigen expression following mRNA-LNP delivery may enable antigen processing through MHC class I presentation pathways. This direct presentation pathway ensures the activation of $CD8^+$ T-cell responses independently of FcγR-mediated uptake of secreted proteins [38]. Thus, antigen presentation to T cells can proceed efficiently through canonical endocytic and antigen-processing mechanisms, independent of FcγR-mediated targeting.

Collectively, these findings indicate that both humoral and cellular arms of adaptive immunity can be engaged in this system. While a robust humoral response is the mandatory requirement for protection against virulent primarily extracellular bacteria such as *Y. pestis* [39,40], the observed priming of cellular immune pathways, typically associated with protection against intracellular pathogens, suggests broader immunomodulatory effects of the Fc-fusion platform beyond antibody production. Notably, such cellular responses may contribute to the clearance of intracellular *Y. pestis*.

Altogether, these findings reframe the utility of Fc in the context of mRNA-LNP vaccines. Rather than acting primarily as a molecular adjuvant through receptor-mediated antigen delivery to antigen-presenting cells, the Fc domain appears to function as a structural and pharmacokinetic scaffold enabling prolonged antigen availability. While contributions of other non-classical Fc receptors or FcRn-dependent antigen recycling cannot be entirely excluded, our findings demonstrate that the enhanced immunogenicity and protection conferred by the F1-based constructs are not primarily driven by FcγR signaling pathways and may involve FcγR-independent mechanisms. The observed effects are broadly consistent with established aspects of Fc biology, although their magnitude may depend on antigen-specific properties such as stability, expression level, and epitope accessibility. Accordingly, although F1 represents a relevant and stringent bacterial vaccine model, these findings should be interpreted within the context of this specific antigen system, and further studies using diverse antigens will be important to better define the generalisability of this Fc-based stabilization strategy.

Taken together, our results provide a mechanistic framework for understanding the role of Fc fusion in F1-based mRNA-LNP vaccines against *Yersinia pestis*. By demonstrating that immunogenicity remains preserved despite species-matching, de glycosylation, or the total absence of classical FcγRs, we show that structural stabilization, rather than xenogeneic recognition or effector function, appears to be the dominant determinant of protective immunity in this model. These findings have broad implications for the design of next-generation mRNA vaccines targeting bacterial pathogens. By leveraging Fc fusion primarily as a pharmacokinetic and structural scaffold, it is possible to enhance immunogenicity without reliance on additional adjuvants or complex antigen designs. Future studies exploring FcRn dependency and the applicability of these principles to other bacterial systems will further refine rational vaccine design. Overall, this work establishes Fc engineering as a versatile and mechanistically informed strategy for optimizing mRNA-LNP vaccine performance, providing a foundation for rapid-response vaccines against high-priority infectious agents. The mechanistic framework proposed here, in which Fc fusion may enhance immunogenicity primarily through antigen stabilization and prolonged systemic availability rather than classical FcγR engagement, may also have broader implications for other vaccine platforms.

4. Materials and methods

4.1. Materials and chemicals

Cholesterol, distearoyl-sn-glycero-3-phosphocholine (DSPC), and dimyristoyl-rac-glycero-3-methoxypolyethylene glycol (PEG-DMG) were from Avanti Polar Lipids (Alabaster, AL, USA). The proprietary ionizable lipid (lipid 14) was synthesized in-house as previously

published [10]. mRNA sequences were synthesized by an *in vitro* transcription (IVT) reaction using the RiboMax T7 transcription kit (Promega) and cleaned by the MEGAclear transcription clean-up kit (Thermo Fisher Scientific). All mRNA sequences were synthesized with complete N1-methyl-pseudouridine nucleotide substitution (Hongene Biotech).

4.2. Design of mRNA constructs

mRNA constructs encoding for the Caf1 antigen were designed as follows: The Caf1 gene (GenBank, account number X61996) section coding for Pro37 to Ser168 was fused to a linker coding for Thr-Gly-Ser-Gly-Asn-Gly followed by Ala22 to Glu36 of the Caf1 gene to generate mF1. SP-F1 encodes for the mF1 protein, with the addition of a 5′ SP sequence originating from the Ig light chain variable region (GenBank, account number U43767.1). All Fc-fusion mRNA constructs were designed as modular fusions composed of the SP-F1 sequence, followed by the sequence coding for the specific Fc constant region scaffold (constant region of human IgG1 adopted from GenBank account number AEV43323.1, IgG4 adopted from GenBank account number AAA03562.1, and mouse IgG2c adopted from GenBank account number CAD60585.1). F1-hIgG1-AG mutant was generated to include the triple mutation (N297G/S298G/T299A) into the hIgG1 scaffold to disrupt the conserved N-linked glycosylation motif. All mRNA constructs included an initiator methionine and a Kozak consensus sequence.

4.3. LNP preparation and characterization

Ionizable lipid, cholesterol, DSPC, and DMG-PEG were mixed at a molar ratio of 40:47.5:10.5:2 with absolute ethanol in a tube. mRNA payloads were suspended in Acetate buffer (25 mm, pH 4.5). To create LNPs, a dual-syringe pump was used to transport the two solutions through the NanoAssembler micromixer from Precision NanoSystem (Vancouver, British Columbia, Canada) at a total flow rate of 12 mL min − 1. The particles were then transferred into dialysis overnight against PBS. Particles in PBS were analyzed for size and uniformity by dynamic light scattering (DLS).

4.4. Cell lines

HeLa cells (American Type Culture Collection, CCL-2) were maintained at 37 °C, 5% CO2 in Dulbecco's modified Eagle's medium supplemented with 10% fetal bovine serum, MEM nonessential amino acids, 2 mM L-glutamine, 1 mM sodium pyruvate, penicillin (100 U/mL) and streptomycin (0.1 mg/mL) (P/S) (Biological Industries, Israel).

4.5. Cell transfection and western blot

One day prior the transfection, HeLa cells (10^5 cells/well) were seeded in 24-well plates (Costar). At the day of the transfection, *in vitro* transcribed and purified mRNA (0.5 μg) coding for the different F1-Fc scaffolds was mixed with Lipofectamine MessengerMax transfection reagent (Invitrogen) and added to each well. Control cells were not transfected. 72 h post-transfection the cells were harvested and the supernatant was separated from the cells by centrifugation. Cell pellets were washed once with phosphate-buffered saline (PBS) and lysed with radioimmunoprecipitation assay (RIPA) lysis buffer (Merck). Equal amounts of protein were resuspended in 1× Laemmli sample buffer (Bio-Rad) supplemented with dithiothreitol (DTT), boiled and resolved by 10% SDS-PAGE. Resolved proteins were blotted to iBlot mini nitrocellulose membranes (Thermo Fisher Scientific). F1 antigen expression was detected using in-house rabbit anti-F1 primary antibodies, followed by fluorophore-conjugated goat anti-rabbit secondary antibodies (IRDye 800CW; LI-COR). Immune complexes were visualized with the ODYSSEY CLx imaging system and analyzed using Image Studio Software (LI-COR).

4.6. Animal models and vaccination experiments

Female C57BL/6JOlaHsd mice (6 to 8 weeks old) were obtained from Harlan (Israel). BALB/c female mice were purchased from Charles River (UK). FcγR KO mice ($mFc\gamma Ra^{null}$) were provided by Prof. Rony Dahan (Department of Systems Immunology, Weizmann Institute of Science, Rehovot, Israel) and maintained in-house [41]. All mice were randomly assigned into cages in groups of 4–8 animals. The mice were allowed free access to water and rodent diet (Harlan, Israel).

The vaccination regimens evaluated in this study consisted of either a single dose or three doses administered at 14-day intervals. For each dose, animals were immunized intramuscularly with 50 μL of vaccine per hind leg (total volume = 100 μL), containing 5 μg of the respective mRNA-LNP formulation or phosphate-buffered saline (PBS) as a negative control. Blood samples were collected from the tail vein prior to each booster dose and before the challenge. For the pharmacokinetic profiles experiment, animals were immunized intravenously with 20 μg/200 μL of the respective mRNA-LNP formulation or phosphate-buffered saline (PBS) as a negative control.

4.7. Anti-F1 enzyme-linked immunosorbent assay

Flat-bottom Maxisorp 96-well microtiter plates (Thermo Fisher Scientific) were coated with 500 ng of purified polymeric F1 (provided by the Biotechnology Department at the Israel Institute for Biological Research) in 50 mM carbonate-bicarbonate buffer (pH 9.6) (Sigma-Aldrich). Following a blocking step with 1× PBS, 2% bovine serum albumin, and 0.05% Tween 20, tested sera were serially diluted in twofold dilutions in a final volume of 50 μl. Alkaline phosphatase-conjugated goat anti-mouse IgG (1/2000 dilution; Sigma-Aldrich) was used as the second layer for anti-F1 IgG titer determination. All incubation steps were performed for 1 h at 37 °C. The plates were extensively washed with 1× PBS and 0.05% Tween 20 before the following step. Titers were defined as the reciprocal values of the end point serum dilutions that displayed optical density at 405 nm (OD_{405}) values twofold higher than the normal serum controls obtained from naïve animals. Enzyme-linked immunosorbent assay (ELISA) analysis was performed in technical duplicates for each animal tested.

4.8. Anti-human Fc IgG1 and anti-mouse Fc IgG2c fragment enzyme-linked immunosorbent assays

Flat-bottom Maxisorp 96-well microtiter plates (Thermo Fisher Scientific) were coated overnight at 4 °C with either purified human IgG1 Fc protein or mouse IgG2c Fc protein (1000 ng and 500 ng per well, respectively) in 50 mM carbonate-bicarbonate buffer (pH 9.6; Sigma-Aldrich). Following a blocking step with 1× PBS, 2% bovine serum albumin, and 0.05% Tween 20, tested sera were serially diluted in twofold dilutions in a final volume of 50 μl. Bound antibodies were detected using alkaline phosphatase-conjugated secondary antibodies (Jackson) specific for the relevant species and immunoglobulin type: donkey anti-mouse IgG (1:2000) or goat anti-mouse IgG light chain-specific antibodies, depending on the assay configuration. For standard curves, alkaline phosphatase-conjugated anti-human Fc IgG1 or rabbit anti-mouse IgG (1:2000; Jackson) were used accordingly. All incubation steps were performed for 1 h at 37 °C. The plates were extensively washed with 1× PBS and 0.05% Tween 20 before the following step. Titers were defined as the reciprocal values of the end point serum dilutions that displayed optical density at 405 nm (OD_{405}) values twofold higher than the normal serum controls obtained from naïve animals. Enzyme-linked immunosorbent assay (ELISA) analysis was performed in technical duplicates for each animal tested.

4.9. Murine interferon-γ Enzyme-Linked Immunosorbent Spot (ELISpot) assay

Mice spleens were dissociated in gentle MACS C tubes (Miltenyi Biotec), filtered, treated with red blood cell lysis buffer (Sigma-Aldrich), and washed. Cell pellets were resuspended in 1 mL of CTL-Test medium (Cellular Technology Limited) supplemented with 1% glutamine and 1 mM penicillin-streptomycin. Single-cell suspensions were seeded in 96-well PVDF plates (4×10^5 cells/well). Splenocytes were stimulated in triplicates with an F1 15-mer peptide library (10 μg/mL; GenScript), concanavalin A (2 μg/mL; Sigma-Aldrich) as a positive control, or CTL medium as a negative control. 24 h post-stimulation, interferon-γ (IFN-γ) secreting cells were quantified using a murine IFN-γ ELISpot kit (Cellular Technology Limited) following the manufacturer's instructions, and spots were counted with an automated ELISpot reader (Cellular Technology Limited).

4.10. Bacterial strain and mouse infection

The fully virulent *Yersinia pestis* strain Kim53 was cultured on brain heart infusion (BHI) agar plates at 28 °C. Colonies were suspended in saline to prepare a bacterial suspension with an OD_{660} of 0.1, corresponding to 1×10^8 CFU/mL. The suspension was serially diluted, and 100 CFU (≈100 LD_{50}) were injected subcutaneously into the lower right back of each mouse. The infectious dose was confirmed by plating diluted suspensions on BHI agar. Mouse survival was monitored daily for 21 days, and sterility of survivors was verified by culturing spleen homogenates on BHI agar supplemented with streptomycin (50 μg/mL) at 28 °C for 48 h.

4.11. Statistical analyses

All values are presented as means + SD/SEM. Statistical analysis was performed using either a one-way analysis of variance (ANOVA) with Tukey's multiple comparisons test (for ELISA data), a two-way ANOVA followed by Bonferroni *post hoc* test (for ELISpot data) and a log-rank (Mantel-Cox) test (for survival data) ($*p < 0.05$, $**p < 0.01$, $***p < 0.001$, and $****p < 0.0001$). Sample sizes (n) are mentioned on each figure captions. Pharmacokinetic parameters for the different mRNA-LNPs were determined non-compartmental analysis in GraphPad Prism 10.6.1. The terminal half-life ($t_{1/2}$) was calculated by fitting the concentration-time data to a non-linear regression model (one-phase decay). Total systemic exposure was quantified as the area under curve (AUC) using the trapezoidal rule (Area Under the Curve analysis) from t_0 to t_{216}. All statistical analyses were performed using GraphPad Prism 10.6.1 statistical software.

CRediT authorship contribution statement

Shani Benarroch: Writing – original draft, Methodology, Investigation, Formal analysis, Data curation. **Hila Cohen:** Methodology, Investigation, Formal analysis. **Uri Elia:** Validation, Investigation. **Yinon Levy:** Investigation, Formal analysis. **Tal Noy-Porat:** Methodology, Investigation, Data curation. **Ronit Rosenfeld:** Validation, Formal analysis. **David Gur:** Methodology, Investigation. **Ron Alcalay:** Methodology, Investigation. **Maya Shlosberg:** Methodology, Investigation, Data curation. **Govinda Reddy Kundoor:** Resources, Methodology, Investigation, Data curation. **Yahel Avraham:** Resources, Methodology, Data curation. **Meir Goldsmith:** Validation, Methodology, Investigation. **Erez Bar-Haim:** Validation, Formal analysis. **Inbal Hazan-Halevy:** Writing – review & editing, Supervision, Investigation. **Ofer Cohen:** Validation, Supervision. **Rony Dahan:** Supervision, Resources. **Emanuelle Mamroud:** Writing – review & editing, Supervision, Project administration. **Dan Peer:** Writing – review & editing, Supervision, Funding acquisition, Conceptualization.

Declaration of competing interest

D.P. receives unrelated licensing fees (to patents on which he was an inventor) from, invested in, consults (or on scientific advisory boards or boards of directors) for, lectured (and received a fee), or conducts sponsored research at TAU for the following entities: ART Biosciences, BioNTech SE, Earli Inc., Kernal Biologics, LAND Therapeutics, Merck KGaA, New Phase Ltd., NeoVac Ltd., RiboX Therapeutics, Roche, SirTLabs Corporation, Teva Pharmaceuticals Inc. The rest of the authors declare no financial interest.

Acknowledgements

This work was partially supported by the European Research Council (ERC advanced grant 101055029), Israel Science Foundation (grant 842/25), the Shmunis Family Foundation, and Lewis Trust all to D.P.

Appendix A. Supplementary data

Supplementary data to this article can be found online at https://doi.org/10.1016/j.jconrel.2026.115555.

Data availability

Data will be made available on request.

References

[1] V. Gote, P.K. Bolla, N. Kommineni, A. Butreddy, P.K. Nukala, S.S. Palakurthi, W. Khan, A comprehensive review of mRNA vaccines, Int. J. Mol. Sci. 24 (2023), https://doi.org/10.3390/ijms24032700.
[2] U. Sahin, A. Muik, E. Derhovanessian, I. Vogler, L.M. Kranz, M. Vormehr, A. Baum, K. Pascal, J. Quandt, D. Maurus, S. Brachtendorf, V. Lörks, J. Sikorski, R. Hilker, D. Becker, A.K. Eller, J. Grützner, C. Boesler, C. Rosenbaum, M.C. Kühnle, U. Luxemburger, A. Kemmer-Brück, D. Langer, M. Bexon, S. Bolte, K. Karikó, T. Palanche, B. Fischer, A. Schultz, P.Y. Shi, C. Fontes-Garfias, J.L. Perez, K. A. Swanson, J. Loschko, I.L. Scully, M. Cutler, W. Kalina, C.A. Kyratsous, D. Cooper, P.R. Dormitzer, K.U. Jansen, Ö. Türeci, COVID-19 vaccine BNT162b1 elicits human antibody and TH1 T cell responses, Nature 586 (2020), https://doi.org/10.1038/s41586-020-2814-7.
[3] N. Pardi, M.J. Hogan, F.W. Porter, D. Weissman, mRNA vaccines-a new era in vaccinology, Nat. Rev. Drug Discov. 17 (2018), https://doi.org/10.1038/nrd.2017.243.
[4] M. Galimand, E. Carniel, P. Courvalin, Resistance of Yersinia pestis to antimicrobial agents, Antimicrob. Agents Chemother. 50 (2006) 3233–3236, https://doi.org/10.1128/AAC.00306-06.
[5] C.E. Demeure, O. Dussurget, G. Mas Fiol, A.S. Le Guern, C. Savin, J. Pizarro-Cerdá, Yersinia pestis and plague: an updated view on evolution, virulence determinants, immune subversion, vaccination, and diagnostics, Genes Immun. 20 (2019), https://doi.org/10.1038/s41435-019-0065-0.
[6] E.E. Galyov, O.Y. Smirnov, A.V. Karlishev, K.I. Volkovoy, A.I. Denesyuk, I. V. Nazimov, K.S. Rubtsov, V.M. Abramov, S.M. Dalvadyanz, V.P. Zav'yalov, Nucleotide sequence of the *Yersinia pestis* gene encoding F1 antigen and the primary structure of the protein. Putative T and B cell epitopes, FEBS Lett. 277 (1990), https://doi.org/10.1016/0014-5793(90)80852-A.
[7] A.V. Karlyshev, E.E. Galyov, V.M. Abramov, V.P. Zav'yalov, Caf1R gene and its role in the regulation of capsule formation of Y. pestis, FEBS Lett. 305 (1992), https://doi.org/10.1016/0014-5793(92)80650-6.
[8] D.A. Chalton, J.A. Musson, H. Flick-Smith, N. Walker, A. McGregor, H.K. Lamb, E. D. Williamson, J. Miller, J.H. Robinson, J.H. Lakey, Immunogenicity of a Yersinia pestis vaccine antigen monomerized by circular permutation, Infect. Immun. 74 (2006), https://doi.org/10.1128/IAI.00437-06.
[9] J.A. Rosenzweig, E.K. Hendrix, A.K. Chopra, Plague vaccines: new developments in an ongoing search, Appl. Microbiol. Biotechnol. 105 (2021), https://doi.org/10.1007/s00253-021-11389-6.
[10] E. Kon, Y. Levy, U. Elia, H. Cohen, I. Hazan-Halevy, M. Aftalion, A. Ezra, E. Bar-Haim, G.S. Naidu, Y. Diesendruck, S. Rotem, N. Ad-El, M. Goldsmith, E. Mamroud, D. Peer, O. Cohen, A single-dose F1-based mRNA-LNP vaccine provides protection against the lethal plague bacterium, Sci. Adv. 9 (2023), https://doi.org/10.1126/sciadv.adg1036.
[11] R.E. Kontermann, Strategies for extended serum half-life of protein therapeutics, Curr. Opin. Biotechnol. 22 (2011), https://doi.org/10.1016/j.copbio.2011.06.012.
[12] D.C. Roopenian, S. Akilesh, FcRn: the neonatal Fc receptor comes of age, Nat. Rev. Immunol. 7 (2007), https://doi.org/10.1038/nri2155.
[13] Z. Shen, C. Li, W. Song, L. Liu, Y. Kong, A. Huang, Q. Bao, T. Ying, Y. Wu, Enhancing vaccine half-life as a novel strategy for improving immune response

durability of subunit vaccines, PLoS Pathog. 21 (2025), https://doi.org/10.1371/journal.ppat.1012845.
[14] T. Noy-Porat, O. Cohen, S. Ehrlich, E. Epstein, R. Alcalay, O. Mazor, Acetylcholinesterase-Fc fusion protein (AChE-Fc): a novel potential organophosphate bioscavenger with extended plasma half-life, Bioconjug. Chem. 26 (2015), https://doi.org/10.1021/acs.bioconjchem.5b00305.
[15] S. Soleimanpour, T. Hassannia, M. Motiee, A.A. Amini, S.A.R. Rezaee, Fcγ1 fragment of IgG1 as a powerful affinity tag in recombinant Fc-fusion proteins: immunological, biochemical and therapeutic properties, Crit. Rev. Biotechnol. 37 (2017), https://doi.org/10.3109/07388551.2016.1163323.
[16] T. Suzuki, A. Ishii-Watabe, M. Tada, T. Kobayashi, T. Kanayasu-Toyoda, T. Kawanishi, T. Yamaguchi, Importance of neonatal FcR in regulating the serum half-life of therapeutic proteins containing the Fc domain of human IgG1: a comparative study of the affinity of monoclonal antibodies and Fc-fusion proteins to human neonatal FcR, J. Immunol. 184 (2010), https://doi.org/10.4049/jimmunol.0903296.
[17] T. Rath, K. Baker, J.A. Dumont, R.T. Peters, H. Jiang, S.W. Qiao, W.I. Lencer, G. F. Pierce, R.S. Blumberg, Fc-fusion proteins and FcRn: structural insights for longer-lasting and more effective therapeutics, Crit. Rev. Biotechnol. 35 (2015), https://doi.org/10.3109/07388551.2013.834293.
[18] F. Junker, J. Gordon, O. Qureshi, Fc gamma receptors and their role in antigen uptake, presentation, and T cell activation, Front. Immunol. 11 (2020), https://doi.org/10.3389/fimmu.2020.01393.
[19] A. Lux, X. Yu, C.N. Scanlan, F. Nimmerjahn, Impact of immune complex size and glycosylation on IgG binding to human FcγRs, J. Immunol. 190 (2013), https://doi.org/10.4049/jimmunol.1200501.
[20] F. Nimmerjahn, J.V. Ravetch, Fcγ receptors as regulators of immune responses, Nat. Rev. Immunol. 8 (2008), https://doi.org/10.1038/nri2206.
[21] D.M. Czajkowsky, J. Hu, Z. Shao, R.J. Pleass, Fc-fusion proteins: new developments and future perspectives, EMBO Mol. Med. 4 (2012), https://doi.org/10.1002/emmm.201201379.
[22] Z. Liu, W. Xu, S. Xia, C. Gu, X. Wang, Q. Wang, J. Zhou, Y. Wu, X. Cai, D. Qu, T. Ying, Y. Xie, L. Lu, Z. Yuan, S. Jiang, RBD-Fc-based COVID-19 vaccine candidate induces highly potent SARS-CoV-2 neutralizing antibody response, Signal Transduct. Target. Ther. 5 (2020), https://doi.org/10.1038/s41392-020-00402-5.
[23] U. Elia, Y. Levy, H. Cohen, A. Zauberman, D. Gur, I. Hazan-Halevy, M. Aftalion, S. Benarroch, E. Bar-Haim, O. Redy-Keisar, O. Cohen, D. Peer, E. Mamroud, Novel bivalent mRNA-LNP vaccine for highly effective protection against pneumonic plague (Adv. Sci. 26/2025), Adv. Sci. 12 (2025), https://doi.org/10.1002/advs.202570206.
[24] S.T. Jung, T.H. Kang, W. Kelton, G. Georgiou, Bypassing glycosylation: engineering aglycosylated full-length IgG antibodies for human therapy, Curr. Opin. Biotechnol. 22 (2011), https://doi.org/10.1016/j.copbio.2011.03.002.
[25] I. Quast, B. Peschke, J.D. Lünemann, Regulation of antibody effector functions through IgG Fc N-glycosylation, Cell. Mol. Life Sci. 74 (2017), https://doi.org/10.1007/s00018-016-2366-z.
[26] M.H. Tao, S.L. Morrison, Studies of aglycosylated chimeric mouse-human IgG. Role of carbohydrate in the structure and effector functions mediated by the human IgG constant region, J. Immunol. 143 (1989), https://doi.org/10.4049/jimmunol.143.8.2595.
[27] X. Wang, M. Mathieu, R.J. Brezski, IgG Fc engineering to modulate antibody effector functions, Protein Cell 9 (2018), https://doi.org/10.1007/s13238-017-0473-8.
[28] A.M. Davies, T. Rispens, P. Ooijevaar-De Heer, H.J. Gould, R. Jefferis, R. C. Aalberse, B.J. Sutton, Structural determinants of unique properties of human IgG4-Fc, J. Mol. Biol. 426 (2014), https://doi.org/10.1016/j.jmb.2013.10.039.
[29] G. Kudla, L. Lipinski, F. Caffin, A. Helwak, M. Zylicz, High guanine and cytosine content increases mRNA levels in mammalian cells, PLoS Biol. 4 (2006), https://doi.org/10.1371/journal.pbio.0040180.
[30] U. Elia, S. Ramishetti, R. Rosenfeld, N. Dammes, E. Bar-Haim, G.S. Naidu, E. Makdasi, Y. Yahalom-Ronen, H. Tamir, N. Paran, O. Cohen, D. Peer, Design of SARS-CoV-2 hFc-conjugated receptor-binding domain mRNA vaccine delivered via lipid nanoparticles, ACS Nano 15 (2021), https://doi.org/10.1021/acsnano.0c10180.
[31] R.M. Martin, J.L. Brady, A.M. Lew, The need for IgG2c specific antiserum when isotyping antibodies from C57BL/6 and NOD mice, J. Immunol. Methods 212 (1998), https://doi.org/10.1016/S0022-1759(98)00015-5.
[32] A.F. Labrijn, T. Rispens, J. Meesters, R.J. Rose, T.H. den Bleker, S. Loverix, E.T. J. van den Bremer, J. Neijssen, T. Vink, I. Lasters, R.C. Aalberse, A.J.R. Heck, J.G. J. van de Winkel, J. Schuurman, P.W.H.I. Parren, Species-specific determinants in the IgG CH3 domain enable fab-arm exchange by affecting the noncovalent CH3–CH3 interaction strength, J. Immunol. 187 (2011), https://doi.org/10.4049/jimmunol.1003336.
[33] W.R. Strohl, Fusion proteins for half-life extension of biologics as a strategy to make biobetters, BioDrugs 29 (2015), https://doi.org/10.1007/s40259-015-0133-6.
[34] R.J. Ober, C.G. Radu, V. Ghetie, E.S. Ward, Differences in promiscuity for antibody-FcRn interactions across species: implications for therapeutic antibodies, Int. Immunol. 13 (2001), https://doi.org/10.1093/intimm/13.12.1551.
[35] W.F. Dall'Acqua, P.A. Kiener, H. Wu, Properties of human IgG1s engineered for enhanced binding to the neonatal Fc receptor (FcRn), J. Biol. Chem. 281 (2006), https://doi.org/10.1074/jbc.M604292200.
[36] M. Pyzik, T. Rath, W.I. Lencer, K. Baker, R.S. Blumberg, FcRn: the architect behind the immune and nonimmune functions of IgG and albumin, J. Immunol. 194 (2015), https://doi.org/10.4049/jimmunol.1403014.
[37] G. Vidarsson, G. Dekkers, T. Rispens, IgG subclasses and allotypes: from structure to effector functions, Front. Immunol. 5 (2014), https://doi.org/10.3389/fimmu.2014.00520.
[38] O.P. Joffre, E. Segura, A. Savina, S. Amigorena, Cross-presentation by dendritic cells, Nat. Rev. Immunol. 12 (2012), https://doi.org/10.1038/nri3254.
[39] J. Hill, S.E.C. Leary, K.F. Griffin, E. Diane Williamson, R.W. Titball, Regions of *Yersinia pestis* V antigen that contribute to protection against plague identified by passive and active immunization, Infect. Immun. 65 (1997), https://doi.org/10.1128/iai.65.11.4476-4482.1997.
[40] A. Amedei, E. Niccolai, L. Marino, M.M. D'Elios, Role of immune response in Yersinia pestis infection, J. Infect. Dev. Ctries. 5 (2011), https://doi.org/10.3855/jidc.1999.
[41] P. Smith, D.J. DiLillo, S. Bournazos, F. Li, J.V. Ravetch, Mouse model recapitulating human Fcγ receptor structural and functional diversity, Proc. Natl. Acad. Sci. USA 109 (2012), https://doi.org/10.1073/pnas.1203954109.